

# THE EFFECT OF NON-UNIFORMITY DENSITY STRUCTURE ON THE MOLECULAR CLOUD-CORES MAGNETIC BRAKING IN THE IDEAL MHD FRAMEWORK

ABBAS EBRAHIMI<sup>\*</sup>, MOHSEN NEJAD-ASGHAR, AZAR KHOSRAVI  
 Department of Physics, University of Mazandaran, Babolsar, Iran

<sup>\*</sup>Corresponding author: [abbas\\_ebri@stu.umz.ac.ir](mailto:abbas_ebri@stu.umz.ac.ir)

Version July 17, 2025

## ABSTRACT

The phenomenon of magnetic braking is one of the significant physical effects of the magnetic field in rotating molecular clouds. The physical characteristics of the core can affect on the core rotation rate. and one of the important parameter is the core density structure. According to observation, by regarding the power-law density distribution,  $r^{-p}$ , for molecular cloud cores, using smoothed particle hydrodynamics simulation, the results show that the increasing of density steepness (i.e., larger  $p$ ) leads to the intensity of the toroidal components of the magnetic field and as a result larger  $B_\phi$ -components lead to more transfer of angular momentum to the outward. Thus, results show that the magnetic braking being stronger with increasing density slope in non-uniform molecular core. For example, the rotation of the system can approximately decrease by fifty percent from  $p = 0.2$  to  $p = 1.8$  for a non-uniform system.

*Subject headings:* stars: formation – ISM: magnetic fields – methods: numerical – ISM: clouds – MHD

## 1. INTRODUCTION

The formation of stars is perhaps one of the least understood and messy processes in cosmic evolution. This process happens in environments that are structured on many scales and are generally referred to as a cloud. Stars are formed in dense regions within the molecular cloud, known as pre-stellar cores, with a density range from  $\geq 10^5 - 10^6 \text{ cm}^{-3}$  at the centre to  $\leq 10^2 \text{ cm}^{-3}$  at the edge, embedded in the clumps (e.g. Myers & Benson 1983; Lada et al. 1993; Williams et al. 1999; Bergin & Tafalla 2007; André et al. 2009; Ferrer Asensio et al. 2022). Dense cores observationally have been thoroughly examined from the molecular spectral line emission (e.g. Benson & Myers 1989; Jijina et al. 1999), infrared absorption (e.g. Teixeira et al. 2005; Lada et al. 2007; Machaieie et al. 2017), and submillimeter dust emission (e.g. Kirk et al. 2005; Marsh et al. 2016). The process of gas collapse that leads to the formation of protostars has been studied for decades. Among the early studies in this field, the works of Larson (1969), Penston (1969) and Shu (1977) can be mentioned. These are generally known as "outside-in" and "inside-out" models, representing the succession of spherical collapse.

Throughout the course of star formation process, various physical mechanisms, such as magnetic field, turbulent, rotation, etc., are influential in the process of star formation and its by-products (i.e., planets). The magnetic field of interstellar environments strongly influences the structure and evolution of the molecular clouds (e.g. Hennebelle & Inutsuka 2019). Observations show that the molecular cloud cores have internal rotations (e.g. Goodman et al. 1993; Ho et al. 1994), considering the magnetic field incorporated with rotation will play a key role in the collapse of the cloud cores, which is known as the "magnetic braking", that arises from the stress caused by the bending of magnetic field lines (e.g. Mestel 1965; Bodenheimer 2011). This mechanism was first investigated by Gillis et al. (1974) to study the transport of angular momentum, from a massive cold gas cloud through the hot galactic background, by the propagation of Alfvén waves. The magnetic braking effect on the evolution of molecular cloud discs and cores was investigated by some pioneer authors (e.g. Mouschovias & Paleologou 1980; Konigl 1987; Basu & Mouschovias 1994). The magnetic braking process is also efficient in the collapse and fragmentation of molecular clouds, which was first investigated by Allen et al. (2003) for a rotating toroidal magnetized core, and by Boss (2007) and Boss (2009) for the collapse and fragmentation of the prolate and oblate molecular clouds. Studies showed that by assuming an ideal MHD and with the magnetic field aligned with the rotational axis of the core, the magnetic braking disrupts the formation of disks around the protostars (e.g. Galli et al. 2006; Mellon & Li 2008). The disk formation depends on two main parameters which control the efficiency of magnetic braking: the ratio of azimuthal and vertical components of the magnetic field at the disk surface, and the Alfvén speed in the surrounding medium. The high efficiency of the magnetic braking and disruption of disk formation around the protostars is known as the magnetic braking catastrophe Galli et al (2009). Three suggestions are presented to resolve the magnetic braking catastrophe: (1) non-ideal MHD effects including ambipolar diffusion (e.g. Mellon & Li 2009; Dapp et al. 2012; Wurster et al. 2016; Zhao et al. 2016, 2018; Lam et al. 2019; Wurster 2021), Ohmic dissipation (e.g. Dapp & Basu 2010; Dapp et al. 2012; Tomida 2015; Wurster et al. 2016; Vaytet et al. 2018), and the Hall effect (e.g. Li et al. 2013; Tsukamoto

2015; Marchand et al. 2018; Zhao et al. 2021), (2) misalignment between rotational axis and magnetic field (e.g. Joos et al. 2012; Li et al. 2013; Krumholz et al. 2013; Codella et al. 2014; Lee et al. 2017; Yen et al. 2021), and (3) turbulence and the dynamical nature of the environment (e.g. Machida et al. 2011; Seifried et al. 2012; Santos-Lima et al. 2012; Seifried et al. 2013; Wurster et al. 2019). Therefore, we can say that the effect of magnetic braking on the formation of protostars and their surrounding disks is completely dependent on the physical characteristics of the core and its surrounding environment, such as density, temperature, turbulence, degree of ionization, geometrical structure of the magnetic field, etc.

One of the important parameter on the magnetic braking catastrophe is the density structure (e.g. Girichidis et al. 2011). Density structures with radial distribution as  $\rho \propto r^{-p}$ , ( $p > 0$ ), are common in systems that have reached intermediate asymptotic states (e.g. Barenblatt 1996; Li & Zhou 2022). The observations made of the galactic molecular clouds MonR2 and NGC 6334 show the steeper density profiles in the galactic arms, and this slope increases in the outer regions of the core clouds (Pirogov 2009; Schneider et al. 2013). The observations of low-mass cores typically show density distributions with  $p$  varying between 1.5 and 2, resembling a finite-size Bonner–Ebert sphere (e.g. Motte & André 2001; Alves et al. 2001; Beuther et al. 2023). Lin et al. (2022) by examining tracers such as  $\text{CH}_3\text{CCH}$ ,  $\text{CH}_3\text{OH}$  and etc. at scales of  $\leq 0.1$  pc obtained a radial profile for the density structure with  $p = 0.25$  to  $p = 1.7$ . Hung et al. (2010) also observationally obtained a  $p$ -value between 1.0 to 1.4 for four cores (Serp-Bolo5, Serp-Bolo1, L158, and Thumbprint Nebula). Kritsuk et al. (2010) simulated a molecular cloud and showed that the density distribution extended as a power-law tail in the star-forming regions. They predicted values from  $p = 7/4$  to  $p = 3/2$  that agree with simulations and observations of star-forming molecular clouds. Observational investigation from the samples of dense cores often suggests slopes  $p \leq 2$  in density profiles for low-mass and high-mass cores (e.g. Hogerheijde & Sandell 2000; Shirley et al. 2002; Young et al. 2003; Beuther et al. 2003; Butler & Tan 2012; Li et al. 2019). Tatematsu et al. (2021) investigated the results of mapping observations containing 107 SCUBA-2 cores in the emission lines of molecules  $\text{N}_2\text{H}^+$ ,  $\text{HC}_3\text{N}$ , and  $\text{CCS}$  at 82 – 94GHz, according to the given mean HWHM radius and beam radius, suggested a power-law index  $p < 1.4$  for the radial density profile. As for the power-law behavior of the density in the core of molecular clouds, one situation that lead to gravitational collapse is  $\rho \propto r^{-2}$  (e.g. Shu 1977; Donkov & Stefanov 2019), while a state like  $\rho \propto r^{-1.5}$  will bring an accretion flow around dense core (e.g. Hoyle & Lyttleton 1941; Bondi 1952). By taking into account the turbulent pressures in the observed linewidth-size scaling, we reach flatter distributions proportional to  $\rho \propto r^{-1}$  in non-isothermal gas (e.g. McLaughlin & Pudritz 1997).

Despite the analytical models presented by assuming a variable density, albeit homologously (e.g. Gillis et al. 1974; Mestel & Paris 1979) and also for example Basu & Mouschovias (1994) who already studied the evolution of a collapsing core with "compact, uniform-density central region, shrinking both in size and mass, surrounded by a 'tail' of matter left behind, in which a near power-law density profile is established", here, we according to the above studies and considering that astrophysical magnetic fields are commonly described using ideal magnetohydrodynamics (MHD), which assumes that the gas is fully ionized, with electrons being tightly coupled to the magnetic field and exhibiting no resistivity, therefore, a tempting question is how does the power law density with different powers affect the magnetic Braking process and core collapse (or, in other words, the formation of a protostar)? For this purpose, in this paper, we consider a power-law density structure with assumption that the magnetic field is proportional to density. We use the PHANTOM simulation code (Price et al. 2018), to study the effect of the density structure on the magnetic braking. In Section § 2, we briefly discuss our numerical methods, model assumptions, and initial conditions. Section § 3 contains the results of our calculations, and the discussion with conclusions are presented in Section § 4.

## 2. METHOD

The ideal MHD equations for the fluid of a prestellar core solved by using a smoothed-particle (magneto)hydrodynamics (SPH) code given by

$$\frac{d\rho}{dt} = -\rho \nabla \cdot \mathbf{v}, \quad (1)$$

$$\frac{d\mathbf{v}}{dt} = -\frac{1}{\rho} \nabla \cdot \left[ \left( P + \frac{B^2}{2\mu_0} \right) \mathbb{I} - \frac{\mathbf{B}\mathbf{B}}{\mu_0} \right], \quad (2)$$

$$\frac{du}{dt} = -\frac{P}{\rho} \nabla \cdot \mathbf{v}, \quad (3)$$

$$\frac{d\mathbf{B}}{dt} = (\mathbf{B} \cdot \nabla) \mathbf{v} - \mathbf{B}(\nabla \cdot \mathbf{v}), \quad (4)$$

where  $\frac{d}{dt} \equiv \frac{\partial}{\partial t} + \mathbf{v} \cdot \nabla$  is the Lagrangian derivative,  $\rho$  is the density,  $\mathbf{v}$  is the velocity,  $u$  is the specific internal energy,  $\mu_0$  is the permeability of free space,  $\mathbb{I}$  is the identity matrix,  $P$  and  $\mathbf{B}$  are thermal pressure and magnetic field, respectively. The density and smoothing length of each SPH particle are calculated iteratively by summing over its nearest neighbours and using  $h = 1.2(\frac{m}{\rho})^{1/3}$  where  $h$ ,  $m$  and  $\rho$  are the SPH particle's smoothing length, mass and density, respectively (e.g. Price & Monaghan 2004). The MHD equations are closed by an equation of state relating the pressure to the density and/or internal energy:

$$P = (\gamma - 1)u, \quad (5)$$

where  $\gamma$  is the adiabatic index.

We set up a dense, cold, spherical, non-uniform density, slowly rotating molecular cloud core of mass  $M = 1M_{\odot}$  and radius  $r_0 = 4 \times 10^{16}$  cm. In this work, we consider, based on observations, the spherical core density, beyond the flattened central region which has a density  $\rho_0^1$  (corresponding to  $n_0 = \rho_0/\mu m_H \sim 10^{10} \text{cm}^{-3}$ ), as following:

$$\rho(r) = \rho_0 \left( \frac{r}{r_0} \right)^{-p}, \quad (6)$$

where  $r \leq r_0$  and  $p > 0$ . This core is placed in pressure equilibrium inside a larger, cubic domain with a side length of  $l = 8 \times 10^{16}$  cm. The density ratio between the core and the warm medium is assumed to be 30 : 1. The sound speed, by assumption a given temperature  $\sim 14\text{K}$ , in the cores is set to  $c_s = 2.18 \times 10^4 \text{km s}^{-1}$ , because the given density profile  $\rho \propto r^{-p}$  cause the density to decrease with radius, while this affects the gas pressure, then, the ratio  $P/\rho$  remains constant, therefore, the sound speed does not vary accross the core. For simplicity, we use periodic but non-self-gravitating boundary conditions on the global domain (Wurster et al. 2016). The core initial rotation is about the z-axis and equal to  $\Omega = 1.77 \times 10^{-13} \text{rad s}^{-1}$ . We assume a magnetic field proportional the density (Crutcher 2012) as follows:

$$B(\rho) = B_0 \left( \frac{\rho(r)}{\rho(r_0)} \right)^{\beta}, \quad (7)$$

where  $B_0$  is a initial magnetic field,  $\beta$  is equal to 0.6, which is the expected scale for conserving magnetic flux during a spherical mass contraction (e.g. see Shu 1992; Myers & Basu 2021).

To calculate the angular velocity of the core we considered a shell of the core. By giving velocity  $(v_x, v_y)$  to all the particles and averaging overall, we obtained an average value for the angular velocity of the shell. We run the models with  $4 \times 10^5$  particles<sup>2</sup>.

### 3. RESULTS

The rotation of the cloud core through the ambient medium bends the magnetic fields, making a  $B_{\phi}$ , which can introduce a force torque to the material in the opposite direction of the core's rotation. As a result, larger  $B_{\phi}$  components lead to more transfer of angular momentum to the outward. In other words, it increases the probability of mass collapse and structure formation. Therefore, in Fig. 1, the toroidal magnetic field ( $B_{\phi}$ ) is plotted at different core radii and for three different times 3K yr, 15K yr, and 40K yr (the period of core rotation is 80k yr), show the uniform and power-law profile density states, respectively.

As seen in Fig. 1, the intensity of the toroidal magnetic field in the inner and middle regions of the core with non-uniform density increases significantly compared to the cores with uniform density. Also, a comparison of two Figures shows that the effect of density changes in the production of toroidal magnetic field in the middle regions of the core appears more in longer times. For example, in 3k yr, the magnetic field in the middle regions is not much different from a core with a uniform density, but after half the core rotation time, the difference between the magnetic fields in the uniform and non-uniform state is very prominent.

In Fig.2 we plot the toroidal magnetic field versus  $B_0$  (initial magnetic field). It is seen that the increasing  $B_0$  leads to increase of toroidal magnetic field component. We know that the toroidal magnetic field and its intensity have a direct effect on the magnetic braking and rotation rate of core. In Fig.3 we show that the rotation rate of core for different values of initial magnetic field for uniform and non-uniform density structures. It is seen that increasing the magnetic field leads to a decrease in the rotation. Also, as we can see in the Fig.3, in the system with power law density model, the reduction of rotation is more than the system with uniform density model.

Noted that, the power index for power-law density typically is taken as  $p = 1.2$ . The results show that, on average, the difference between two mentioned models is approximately 25 percent. At follow, we examined the power law density model with different values of  $p$ -index. Results are shown in Fig.4. It is seen that power law models with larger  $p$  values lead to faster reduction of core rotation. It can be concluded that the magnetic braking effect increases in such models. The toroidal magnetic field has a direct effect on the magnetic braking, so we can conclude that the increasing  $p$ -index leads to an increase in the toroidal magnetic field. This result is also shown in Fig.5.

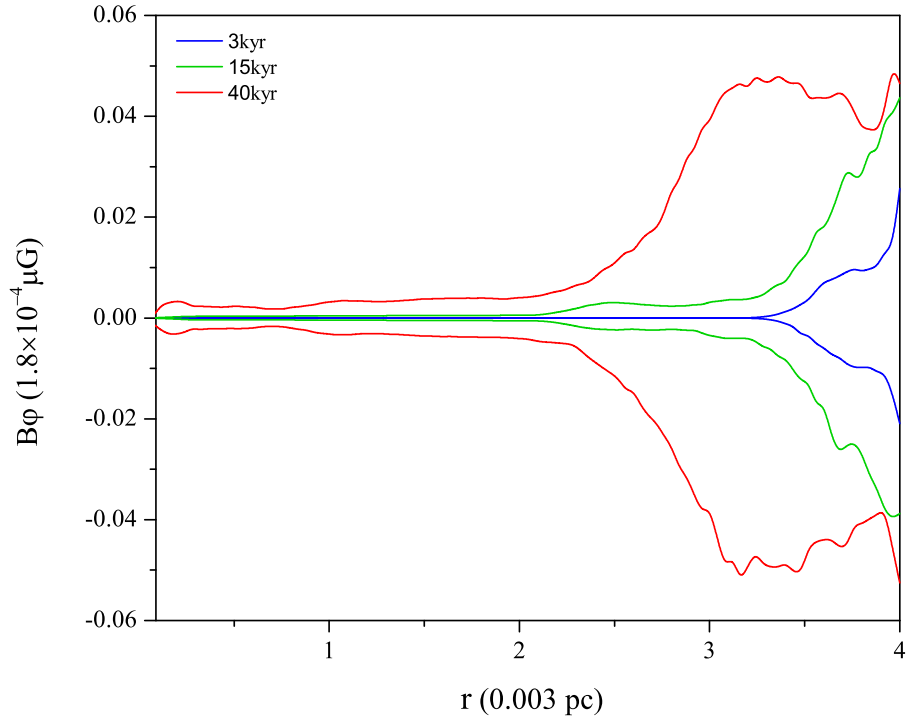
### 4. CONCLUSION

In this paper, we studied the magnetic braking effect in the core of quasi-static molecular clouds. To investigate this issue, we used SPH numerical simulation. In the studied models, it was assumed that the density of the cores is uniform. However, there is observational evidences that the density inside the core can be non-uniform (e.g. Barenblatt 1996). This led us to investigate the effect of the non-uniform density of the molecular cloud core on the magnetic braking effect. For this purpose, we considered a power-law model for the core density as  $\rho(r) = \rho_0(r/r_0)^{-p}$  where the  $p$ -index in a way indicates the degree of non-uniformity.

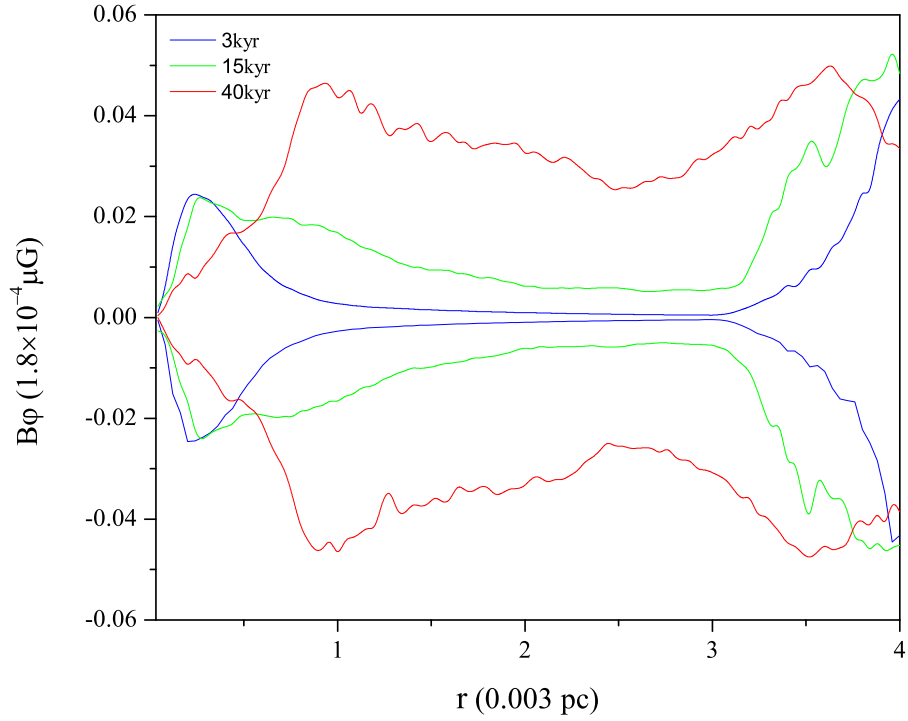
According to the results, we found that the toroidal magnetic field in non-uniform systems has larger values than in the uniform density case, and increasing  $p$  (the amount of non-uniformity) further increases the toroidal magnetic field intensity (Fig.1 and 5). Also, the result show that the toroidal magnetic field have larger value in the outer radius of core in uniform density system. However, it can be said that in systems with non-uniform density, the magnetic field

<sup>1</sup> The central density is calculated according to the Plummer-like model for the inner regions of the core (e.g. Auddy et al. 2019).

<sup>2</sup> By investigating a higher resolutions, finding that it has a negligible impact on our results, about 2%



(a)



(b)

FIG. 1.— The toroidal magnetic field as a function of radius for initial magnetic field  $B_0 = 30 \mu\text{G}$ , mass  $1M_\odot$ , and three times: 3 K yr (green), 15 K yr (blue) and 40 K yr (red) for (a) a core with uniform density  $\rho_0$  and (b) a core with non-uniform density in power-law model with  $p = 1.2$ .

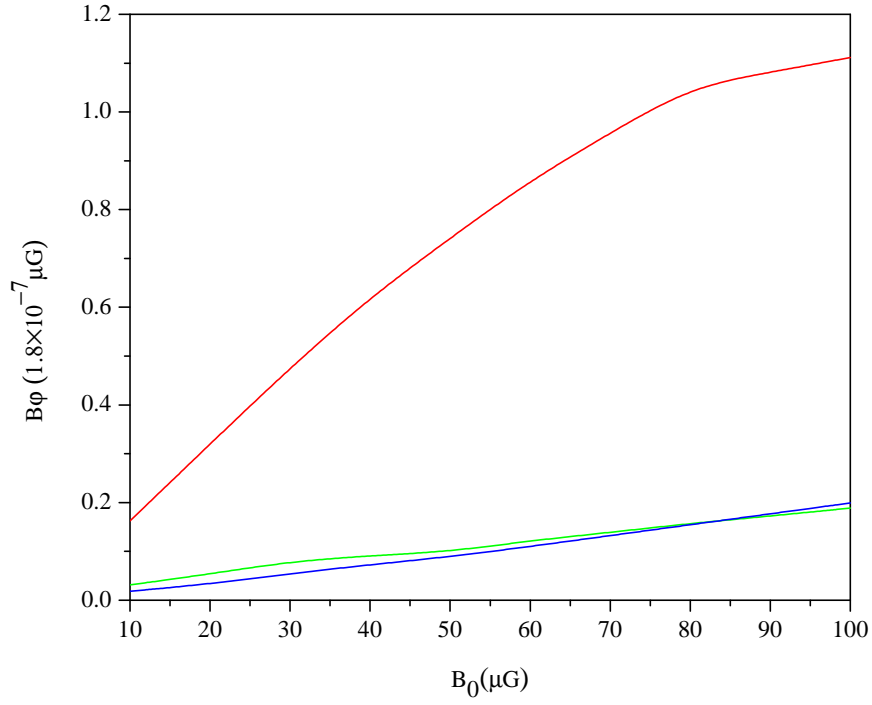


FIG. 2.— The toroidal magnetic field,  $B_\phi$ , as a function of different initial magnetic field values,  $B_0$ , for a  $1M_\odot$  core with power-law index  $p = 1.2$  after 15Kyr time, at radii of  $5.4 \times 10^{-3}$  (blue),  $8.4 \times 10^{-3}$  (green), and  $11.4 \times 10^{-3}$ pc (red) .

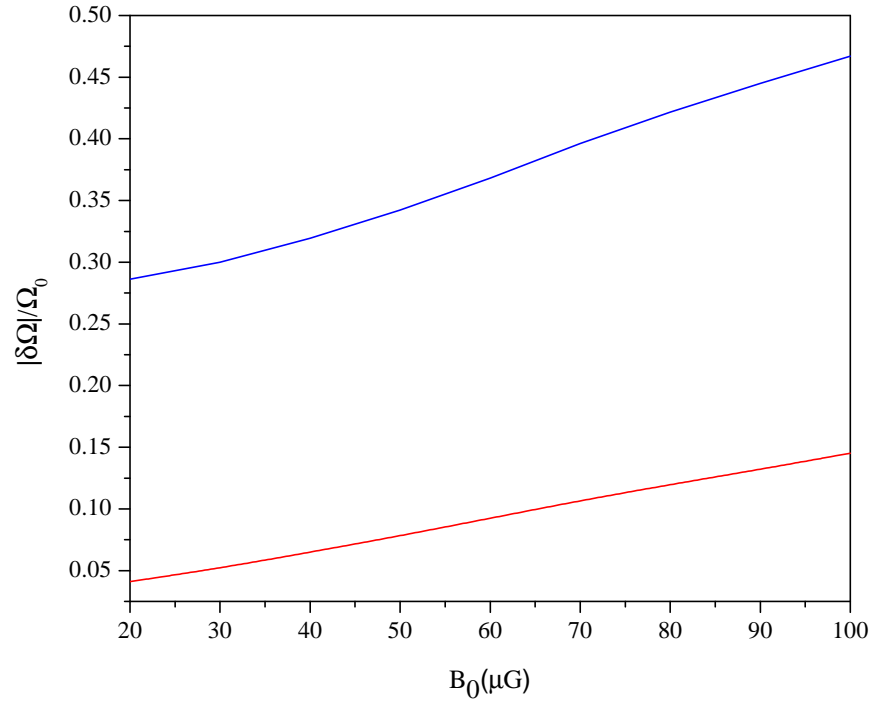


FIG. 3.— The relative changes of the rotation for a uniform (red) and non-uniform (blue) density, with  $p$ -index 1.2, core as a function of initial magnetic field,  $B_0$ , over 40Kyr .

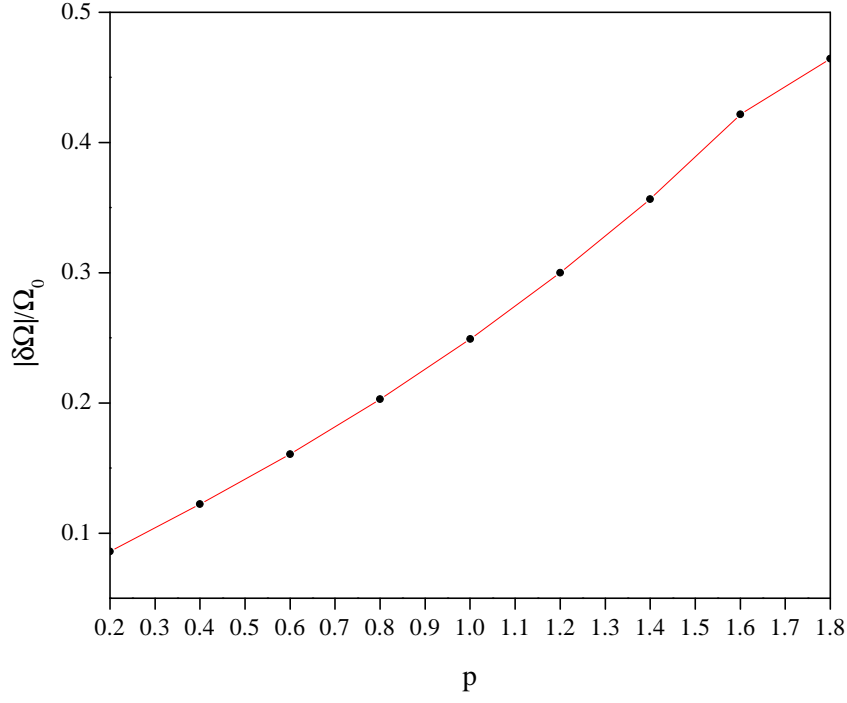


FIG. 4.— The relative changes of the rotation for a non-uniform density core, with  $B_0 = 30\mu\text{G}$  and mass  $1M_\odot$ , as a function of different values of  $p$ -index at 40K yr.

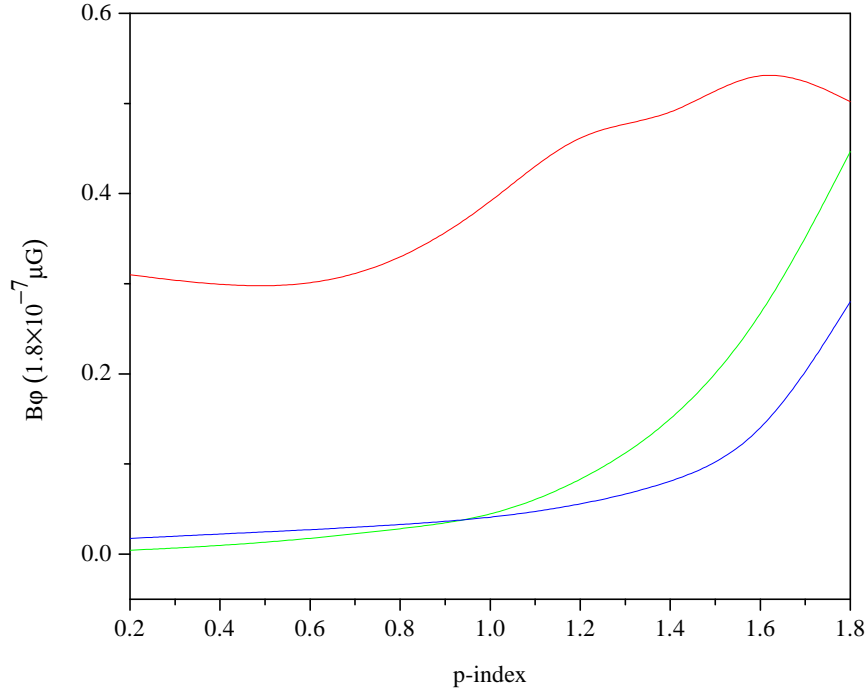


FIG. 5.— The toroidal magnetic field,  $B_\phi$ , as a function of different  $p$ -index values, for a  $1M_\odot$  core over a 15K yr period, shown for radii of  $5.4 \times 10^{-3}$  (green),  $8.4 \times 10^{-3}$  (green), and  $11.4 \times 10^{-3}\text{pc}$  (red).

has a significant value in all radii. The Fig.2 Show that the value of toroidal magnetic field is dependent on the initial magnetic field of cloud,  $B_0$ . The bigger value of  $B_0$ , leads to bigger toroidal magnetic field in the core. According to Crutcher 2012 we know that  $B \propto \rho^\beta$  where  $\beta = 0.6$ . Clouds with greater value of density have a larger initial and so larger toroidal component magnetic field.

In Fig.1, for a uniform initial density, we see that the magnetic field in the outer regions increases with time. Therefore, we can conclude that after a certain period of time, the uniformity of the density of the system is lost and the outer regions have higher densities than the inner regions. However, as can be seen for non-uniform model, the magnetic field in the inner and outer regions does not differ much, and the gradient of the field becomes smoother with the radius. Therefore, according to the relationship between field and density, we can conclude that after a certain period of time, the density gradient of the system becomes smoother too. On the other hand, as we have already mentioned, the increase of the toroidal magnetic field leads to the increase of magnetic braking effect. This is because of the magnetic lined become twisted and the twist propagate outward along the field line at the Alfvén velocity. The barking time is given as  $t_b \propto \rho/V_A$  where  $V_A$  is the Alfvén speed that is proportional to  $B^2$  and the analytical study showed that  $\Omega(t) \propto \exp(-t/t_b)$  (e.g. Bodenheimer 2011). Therefore, the rotation speed of the system should be reduced.

In Fig.3, the relative changes of the rotation speed are plotted in terms of the initial field for uniform (red line) and non-uniform density (blue line). It can be seen that the rotation of the system or in other words the angular momentum of the system in the non-uniform state is significantly reduced compared to the uniform state. The results show that, on average, the difference between two mentioned models is approximately %25 for  $p = 1.2$ . Also, Fig.4 shows that if the degree of non-uniformity of the system,  $p$ , increases, the rate of decline of the rotation of the system increases. For example, the rotation of the system can approximately decrease by %50 from  $p = 0.2$  to  $p = 1.8$  for a non-uniform system.

In general, it can be said that in the uniform density case, the  $B_\phi$  magnetic field components appear in the outer regions of the core, and the decrease in core rotation in this case is less than in the non-uniform case where we have a  $B_\phi$  component throughout the core. The rate of decrease in core rotation in the non-uniform model depends on  $p$ , and in this presented model, for  $p = 1.2$ , about %25 decreased. For the power-law density profile, the potential and gravitational force change with distance much more slowly than for a point mass. This could indicate that the environment of the cores is probably gravitationally bound to them (e.g. Kirk et. al. 2017) that in turn could be a confirmation of more efficiency on magnetic braking.

## REFERENCES

- Allen, A., Li, Z.-Y., Shu F. H., 2003, *ApJ*, **599**, 363
- Alves, J. F., Lada, C. J., & Lada, E. A. 2001, *Nature*, **409**, 159
- André, P., Basu, S., & Inutsuka, S., 2009, in *The Formation and Evolution of Prestellar Cores*, ed. G. Chabrier (Cambridge: Cambridge Univ. Press), 254
- Auddy, S., Myers, P. C., Basu, S., et al. 2019, *ApJ*, **872**, 207
- Barenblatt, G. I., 1996, *Scaling, self-similarity, and intermediate asymptotics: dimensional analysis and intermediate asymptotics*, Cambridge University Press
- Basu, S., & Mouschovias, T. C. 1994, *ApJ*, **432**, 720
- Benson, P. J., & Myers, P. C. 1989, *ApJS*, **71**, 89
- Bergin, E. A., & Tafalla, M., 2007, *ARA&A*, **45**, 339
- Beuther H., Schilke P., Menten K. M., et al. 2002, *ApJ*, **566**, 945
- Beuther, H., Gieser, C., Soler, J. D., et al. 2023, *A & A*, **682**, 23
- Bodenheimer, P. H. 2011, *Principles of Star Formation* (2nd ed.; Berlin: Springer)
- Bondi H. 1952, *MNRAS*, **112**, 195
- Boss, A. P. 2007, *ApJ*, **685**, 1136
- Boss, A. P. 2009, *ApJ*, **97**, 1940
- Butler M. J., & Tan J. C. 2012, *ApJ*, **754**, 5
- Codella, C., Cabrit, S., Gueth, F., Podio, L., Leurini, S., Bachiller, R., Gusdorf, A., Lefloch, B., & Nisini, B. 2014, *A & A*, **568**, L5
- Crutcher, R. M. 2012, *ARA&A*, **50**, 29
- Donkov, S., & Stefanov, I. 2019, *MNRAS*, **485**, 3224
- Dapp, W. B., & Basu, S. 2010, *A & A*, **521**, 4
- Dapp, W. B., Basu, S., & Kunz, M. W. 2012, *A & A*, **541**, 18
- Ferrer Asensio, J., Spezzano, S., Caselli, P., et al. 2022, *A&A*, **667**, A119
- Galli, D., Lizano, S., Shu, F. H., & Allen, A. 2006, *ApJ*, **647**, 374
- Galli, D., Cai, M., Lizano, S., & Shu, F. H. 2009, *RMxAC*, **36**, 143
- Gillis, J., Mestel, L., & Paris, R. B. 1974, *Ap & SS*, **27**, 167
- Girichidis, P., Federrath, C., Banerjee, R., & Klessen, R. S. 2011, *MNRAS*, **413**, 2741
- Goodmann, A. A., Benson, P. J., Fuller, G. A., & Myers, P. C. 1993, *ApJ*, **406**, 528
- Hennebelle, P., & Inutsuka, S.-i. 2019, *Frontiers in Astronomy and Space Sciences*, **6**, 5
- Ho, P. T. P., Terebey, S., & Turner, J. L. 1994, *ApJ*, **423**, 320
- Hogerheijde M. R., & Sandell G. 2000, *ApJ*, **534**, 880
- Hoyle F., & Lyttleton R. A. 1941, *MNRAS*, **101**, 227
- Hung, C.-L., Lai, S.-P., & Yan, C.-H. 2010, *ApJ*, **710**, 207
- Jijina, J., Myers, P. C., & Adams, F. C., 1999, *ApJS*, **125**, 161
- Joos, M., Hennebelle, P., & Ciardi, A. 2012, *A & A*, **543**, 22
- Kirk, J. M., Ward-Thompson, D., & André, P., 2005, *MNRAS*, **360**, 1501
- Kirk, H., Friesen, R. K., Pineda, J. E., et al. 2017, *ApJ*, **846**, 144
- Konigl, A. 1987, *ApJ*, **320**, 726
- Kritsuk, A. G., Norman, M. L., & Wagner, R. 2010, *ApJL*, **727**, L20
- Krumholz, M. R., Crutcher, R. M., & Hull, C. L. H. 2013, *ApJL*, **767**, L11
- Lada, E. A., Strom, K. M., & Myers, P. C., 1993 in *Protostars and Planets III*, ed. E. H. Levy & J. I. Lunine, 245
- Lada, C. J., Alves, J. F., & Lombardi, M. 2007, in *Protostars and Planets V*, ed. B. Reipurth, D. Jewitt, & K. Keil (Tucson, AZ: Univ. Arizona Press), 3
- Lam, K. H., Li, Z. -Y., Chen, C. -Y., Tomida, K., & Zhao, B. 2019, *MNRAS*, **482**, 5326
- Larson, R. B., 1969, *MNRAS*, **145**, 271
- Lee, C.-F., Li, Z.-Y., Ho, P. T. P., Hirano, N., Zhang, Q., & Shang, H. 2017, *Sci. Adv.*, **3**, e1602935
- Li, Z.-Y., Krasnopolsky, R., & Shang, H. 2013, *ApJ*, **774**, 12
- Li, S., Zhang, Q., Pillai, T., et al. 2019, *ApJ*, **886**, 130
- Li, G. X., Zhou, J. X., 2022, *MNRAS*, **514**, L16
- Lin, Y., Wyrowski, F., Liu, H. B., et al. 2022, *A&A*, **658**, A128
- Machaieie, D. A., Vilas-Boas, J. W., Wuensche, C. A., Racca, G. A., Myers, P. C., & Hickel, G. R., 2017, *ApJ*, **836**, 19
- Machida, M. N., Inutsuka, S.-I., & Matsumoto, T. 2011, *PASJ*, **63**, 555
- Marchand, P., Commerçon, B., & Chabrier, G. 2018, *A & A*, **619**, 16
- Marsh, K. A., Kirk, J. M., André, P., et al. 2016, *MNRAS*, **459**, 342
- McLaughlin, D. E., & Pudritz, R. E. 1997, *ApJ*, **476**, 750
- Mellon, R. R., & Li, Z.-Y. 2008, *ApJ*, **681**, 1356
- Mellon, R. R., & Li, Z.-Y. 2009, *ApJ*, **698**, 922
- Mestel, L. 1965, *QJRAS*, **6**, 161
- Mestel, L., & Paris, R. B. 1979, *MNRAS*, **187**, 337
- Motte, F., & André, P. 2001, *A & A*, **365**, 440
- Mouschovias, T. C., & Paleologou, E. V. 1980, *ApJ*, **237**, 877
- Myers, P. C., & Basu, S. 2021, *ApJ*, **917**, 35
- Myers, P. C., & Benson, P. J., 1983, *ApJ*, **266**, 309
- Penston, M. V., 1969, *MNRAS*, **144**, 425
- Price D. J., & Monaghan J. J. 2004, *MNRAS*, **348**, 139
- Price, D. J., Wurster, J., Tricco, T. S., et al. 2018, *PASA*, **35**, e031
- Pirogov, L. E. 2009, *Astronomy Reports*, **53**, 1127
- Santos-Lima, R., de Gouveia Dal Pino, E. M., & Lazarian, A. 2012, *ApJ*, **747**, 21
- Schneider, N., André, P., Konyves, V., et al. 2013, *ApJL*, **766**, L17
- Seifried, D., Banerjee, R., Pudritz, R. E., & Klessen, R. S. 2012, *MNRAS*, **423**, L40
- Seifried, D., Banerjee, R., Pudritz, R. E., & Klessen, R. S. 2013, *MNRAS*, **432**, 3320
- Shirley Y. L., Evans Neal J. I., & Rawlings J. M. C. 2002, *ApJ*, **575**, 337
- Shu, F. H. 1992, in *Physics of Astrophysics*, Vol. II, ed. F. H. Shu (Mill Valley, CA: Univ. Science Books)
- Shu F. H., 1977, *ApJ*, **214**, 488
- Tatematsu, K., Kim, G., Liu, T., et al. 2021, *ApJS*, **256**, 25
- Teixeira, P. S., Lada, C. J., & Alves, J. F., 2005, *ApJ*, **629**, 276
- Tomida, K., Okuzumi, S., & Machida, M. N. 2015, *MNRAS*, **801**, 20
- Tsukamoto, Y., Iwasaki, K., Okuzumi, S., Machida, M. N., & Inutsuka S. 2015a, *MNRAS*, **452**, 278
- Vaytet, N., Commerçon, B., Masson J., González, M., & Chabrier, G. 2018, *A & A*, **615**, 18
- Williams, J.P., Blitz, L., & McKee, C.F., 1999, *Protostars and Planets IV*, P. 97
- Wurster, J., Bate, M. R., & Price, D. J. 2016, *MNRAS*, **457**, 1037
- Wurster, J., Bate, M. R., & Price, D. J. 2019, *MNRAS*, **489**, 1719
- Wurster, J. 2021, *MNRAS*, **501**, 5873
- Yen, H.-W., Koch, P. M., Hul, C. L. H., Ward-Thompson, D., Bastien, P., Hasegawa, T., Kwon, W., Lai, S.-P., Qiu, K., & Ching, T.-C. 2021, *ApJ*, **907**, 33
- Young C. H., Shirley Y. L., Evans Neal J. I., & Rawlings J. M. C. 2003, *ApJS*, **145**, 111
- Zhao, B., Caselli, P., Li, Z. -Y., Krasnopolsky, R., Shang, H., & Nakamura, F. 2016, *MNRAS*, **460**, 2050
- Zhao, B., Caselli, P., Li, Z. -Y., Krasnopolsky, R. 2018, *MNRAS*, **473**, 4868
- Zhao, B., Caselli, P., Li Z. -Y., Krasnopolsky, R., Shang, H., & Lam, K. H. 2021, *MNRAS*, **505**, 5142